Physicochem. Probl. Miner. Process., 55(5), 2019, 1070-1081

http://www.journalssystem.com/ppmp

Physicochemical Problems of Mineral Processing

ISSN 1643-1049

Received December 29, 2018; reviewed; accepted April 26, 2019

Ammonium chloride's weakening effect on the copper activation of pyrite in flotation and the surface regulation mechanism behind it

Shengdong Zhang, Yumeng Chen, Xiong Tong, Xian Xie, Yalin Lu

Faculty of Land Resource Engineering, Kunming University of Science and Technology, Kunming 650093, China

Corresponding authors: kgxiongtong@163.com (Xiong Tong), xianxie2008@kmust.edu.cn (Xian Xie)

Abstract: The traditional separation process of pyrite and marmatite is carried out under highly alkaline conditions. Therefore, a large amount of lime is demanded and the zinc recovery cannot be guaranteed. However, under weakly alkaline conditions, copper-activated pyrite has good floatability, which is difficult to separate from marmatite. In this paper, ammonium chloride (NH_4Cl) is used for depressing the flotation of copper-activated pyrite to achieve the separation of these two minerals under weakly alkaline environment. The flotation tests show that NH_4Cl can significantly reduce the floatability of pyrite in weakly alkaline conditions. The results of adsorption tests and X-ray photoelectron spectroscopy (XPS) analyses indicate that NH_4Cl can obviously change the composition of pyrite surface by increasing the content of iron/copper hydroxide and reducing the content of copper sulfides. Calculation of the solution composition demonstrates that the addition of NH_4Cl results in the occurrence of $Cu(NH_3)_n^{2+}$ and the pH buffering property. Based on these results, it can be concluded that the depression of NH_4Cl on copper activated pyrite is mainly derived from two aspects: 1) the pH buffering property of the conjugated acid-base pair (NH_4^+/NH_3) can impede the decline of OH^- concentration, which results in more hydroxide adsorbed on pyrite; 2) $NH_3(aq)$ competes with the pyrite surface to consume Cu^{2+} through complexation, which causes a reduction in the amount of copper sulfides formed on the pyrite surface.

Keywords: pyrite, depression, cuprammonium solution, pH buffering property, flotation

1. Introduction

Pyrite (FeS_2) is the most common sulfide mineral and it is usually associated with zinc sulfide minerals (Jiang et al., 1998). The removal of pyrite from zinc sulfide minerals is necessary to meet the requirements of subsequent metallurgy (Ahmadi et al., 2012). But there are some technical difficulties in this beneficiation process. In order to improve the separation efficiency, a large amount of lime is demanded to maintain the highly alkaline of pulp, which could lead to pipe scaling and the floatability of marmatite significantly decreased (Shen et al., 1998). Because the adsorption of iron hydroxide and zinc hydroxide could reduce the hydrophobicity of marmatite (Shen et al., 2001; Boulton et al., 2005; Qin et al., 2012). When reducing the pH, the recovery of zinc sulfide minerals is improved, and lime consumption is drastically reduced. The flotation separation of pyrite and zinc sulfide minerals in a weakly alkaline environment becomes a choice worth exploring.

Under weakly alkaline conditions, the insufficient depression of pyrite leads to its transportation into zinc concentrate. Hence, many researchers have made various attempts to improve the flotation selectivity. These works can be summarized in two aspects: searching for new selective collectors to reduce the collection of pyrite (Shen et al., 1998; Buckley et al., 2014); looking for more effective depression methods of pyrite to prevent collector adsorption (Peng et al., 2012; Bulut et al., 2012). The most frequently studied selective collectors are mainly thionocarbamate and thiourea-type collectors (Shen et al., 1998; Buckley et al., 2014). These collectors, chemisorb on copper sulfides through chelation between the S/O of the collector and Cu on the mineral surface (Buckley et al., 2014), but physically

DOI: 10.5277/ppmp19029

adsorb on pyrite surface. However, xanthate could chemically adsorb on the surface of both copper sulfide minerals and pyrite (Deng et al., 2013). Hence, these collectors exhibit higher selectivity against pyrite than xanthate. However, in weakly alkaline environment, copper activation could lead to the formation of $CuFeS_2$-type layer on pyrite surface, which decreases the selectivity of these collectors (Ejtemaei and Nguyen, 2017). Regarding the depression of pyrite, adding depressants and controlling the Eh value by gas purging have been adopted (Boulton et al., 2001; Guo et al., 2015). For the depressants, both inorganics (cyanide, sulfoxyl reagents, etc.) (Guo et al., 2015; Dávila-Pulido et al., 2011) and organics (polysaccharides, polyacrylamides, modified lignosulfonate biopolymers, diethylenetriamine, etc.) (Bicak et al., 2007) have been applied. However, there are various defects in these depression methods. Gas purging is time consuming and its industrial feasibility is low (Boulton et al., 2001). High dosages of sulfoxyl reagents lead to high costs (Bulut et al., 2012). Cyanide is harmful for the environment and poisonous for humans (Mehrabani et al., 2011). Organic depressants usually have poor selectivity and need a modification in structure. Therefore, the separation of zinc sulfide minerals and pyrite under weakly alkaline environments still need to be studied.

Copper activation, could result in a significant increase in pyrite floatability within the pH range of 6-10 (Valdivieso et al., 2004), and it should be responsible for the deterioration of the separation of pyrite and zinc sulfide minerals under weakly alkaline environment. Therefore, weakening the copper activation of pyrite is the key to achieve separation in weakly alkaline conditions. The ammonia molecule has a great affinity for copper ions (Bidariand Aghazadeh, 2015) and the observation of Xiaojun and Kelebek (2000) has demonstrated that ammonium salts can hinder the flotation of copper-activated pyrite, so adding NH_4Cl into the flotation system to regulate the copper activation of pyrite has been studied here. In this paper, microflotation tests are carried out to assess the effect of NH_4Cl on the separation of marmatite and pyrite. The weakening effect of NH_4Cl on copper activation of pyrite is further studied through adsorption tests, XPS analyses and the calculation of solution equilibrium.

2. Experimental

2.1. Materials and reagents

The pure pyrite and marmatite samples are obtained from the Chi Hong Mine, Yunnan Province, China. After the manual removal of gangue minerals such as quartz and calcite, the samples are dry-ground in a porcelain ball mill and dry-screened to obtain the size fraction of -0.075 mm ~ + 0.044 mm. The samples are packed and sealed under an atmosphere of N_2 in nitrogen storage cabinet (DQ, Yongheng Experimental instrument factory, China). The chemical compositions of the samples are given in Table 1 and the XRD spectra are shown in Fig. 1. The results of chemical and the XRD spectra indicate that both marmatite and pyrite samples have high purity. Before conducting the experiments, the pure mineral samples are scrubbed under ultrasonication (25 °C, 40 KHz, 150 w) for 5 min and then washed three times with deionized water to obtain fresh and consistent mineral surface.

The water is purified through an ultra-pure water machine (UPT–I–10T, ULUPURE, China) with a reverse osmosis RIO unit to obtain the Milli-Q water with a resistance of 18.2 $M\Omega \cdot cm^{-1}$ for experimental use. The pH is measured with a high precision pH meter (PHS-3C, Shenzhen Liang yi Laboratory Instrument Co., Ltd., China). The $CuSO_4 \cdot 5H_2O$ (activator), NH_4Cl (activator), HCl/NaOH (pH adjuster), $Na_2B_4O_7 \cdot 10H_2O$ (pH buffering agent) and $C_{10}H_{14}N_2Na_2O_8$ (disodium EDTA) (extractant) used in the experiment are all of analytical purity. The potassium n-butyl xanthate (KBX) is purified by dissolving it in acetone and then recrystallizing it from ether (Leppinen, 1990).

Table 1. The chemical compositions of marmatite and pyrite sample

Element	Zn	S	Fe	Pb	Cu	Si	CaO	MgO
Content in marmatite (%)	57.68	32.91	8.51	0.025	0.039	0.47	0.15	0.12
Content in pyrite (%)	-	52.86	46.13	0.046	0.051	0.59	0.11	0.16

2.2. Flotation tests

The flotation tests are conducted in a modified Hallimond tube (see Fig. 2) with 1 g pyrite sample for each test (1 g pyrite and 1 g marmatite for the mixed flotation). After cleaning, the sample is conditioned

by magnetic stirring (800 rpm) for 5 min in 40 mL activator solution. The pH of the activator solution is adjusted by adding 0.01 mol/L NaOH or 0.01 mol/L HCl in advance. The sample is then conditioned for another 2 min with 10 mg/L of KBX. After that, flotation is performed for 10 min (2/4/6/8 min for the mixed flotation) with an air-flow rate of 0.010 L/min. After flotation is completed, the floated and nonfloated fractions are filtered, dried at 40 °C, and then weighed to calculate the recovery. For the mixed flotation, the recovery is calculated based on the product grades assessed by chemical analyses. Each test is repeated three times, and the average recovery is calculated for final reporting. The standard deviation in the figure reflects the error of the experimental data.

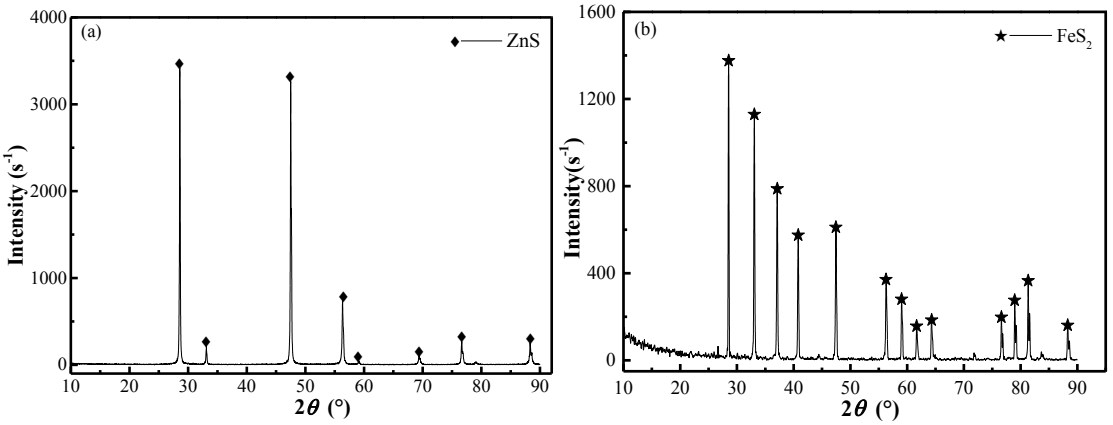

Fig. 1. XRD analyses spectra of (a) marmatite and (b) pyrite

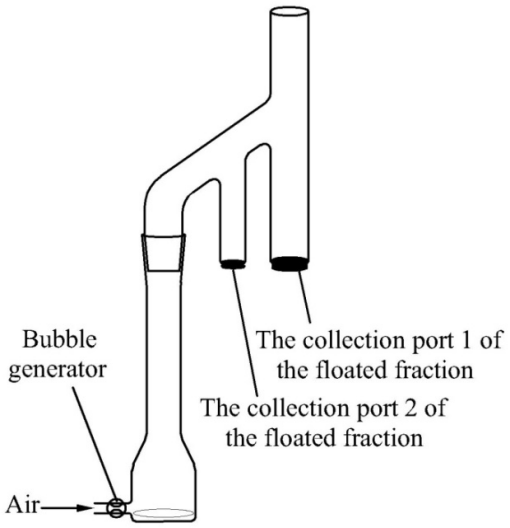

Fig. 2. The schematic diagram of the modified Hallimond tube

2.3. Adsorption tests

The adsorption amounts of copper and KBX on the pyrite surface are measured by the residual concentration method. Additionally, disodium EDTA is used to selectively extract copper and iron hydroxides adsorbed on the pyrite surface to determine their amounts (Rumball et al., 1996; He et al., 2005). 1 g pyrite is conditioned in copper sulfate (5×10^{-5} mol/L $CuSO_4$) or cuprammonium solution (CAS, which is prepared by mixing the copper sulfate and NH_4Cl solution in advance.) for 5 min at pH = 9. After conditioning, the suspension is filtered, and the filtrate is stored as 'Sample No. 1'. The filter residueis extracted using 3 wt% disodium EDTA solution for 20 min. The suspension is filtered when the extraction is finished, and the filtrateis stored as 'Sample No. 2'. Before the extraction, nitrogen is purged in the disodium EDTA solution to prevent the oxidation of pyrite. The extraction is performed at pH = 9.

The total amount of copper adsorbed and the amount of extracted and unextracted copper on the pyrite surface can be calculated using the following equations,

$$\Gamma_{\text{total}} = (C_0 - C_1)\, V_1 / (M * SA) \quad (1)$$

$$\Gamma_{\text{extracted}} = C_2 V_2 / (M * SA) \quad (2)$$

$$\Gamma_{\text{unextracted}} = \Gamma_{\text{total}} - \Gamma_{\text{extracted}} \quad (3)$$

where C_0, C_1, and C_2 are the initial copper concentration, the copper concentration of Sample No. 1 and that of Sample No. 2, respectively. V_1 and V_2 are the volume of the activation solution and the disodium EDTA solution, respectively. *M* is the mass of the mineral sample used in each adsorption test. *SA* is the specific surface area of the pyrite sample used in this study, which is determined by the Brunnauer–Emmett–Teller (BET) technique and is found to be 0.048 m^2/g. The amount of extracted iron can also be calculated using Eq. (2). However, in this case, C_2 is the ion concentration of Sample No. 2. The copper and iron concentration are measured by inductively coupled plasma atomic emission spectrometry (ICP-AES) (ICPS-1000II, Shimadzu, Japan).

For the measurement of the KBX adsorption amount, 1g pyrite is firstly conditioned in the corresponding activation solution for 5 min, and then, the supernatant is discarded. The remaining solid sample is conditioned in the KBX solution for another 2 min. After that, the suspension is filtered, and the residual concentration of KBX in the filtrate is measured using a 751 UV-vis spectrophotometer (Inesa Analytical Instrument Co., Ltd., Shanghai, China). During the test, the wavelength of light is fixed at the maximum absorption wavelength of KBX (301 nm) (Leppinen, 1990). The adsorption amount of KBX can be calculated using Eq. (1). In this case, C_0 is the initial concentration of KBX, C_1 is the residual concentration of KBX in the filtrate and V_1 is the volume of KBX solution. Measurement under each condition is performed in triplicate. The experimental errors of the adsorption amount are quantified though the standard deviation.

2.4. XPS analyses

XPS analyses are used to identify the species present on the surface of pyrite conditioned in different solutions. A spectrometer (PHI5000 Versa probe II, ULVAC–PHI, Japan) equipped with a monochromatic Al K X–ray source with a passenergy of 46.95 eV is used to carry out the measurement. The analyses are carried out at room temperature with a pressure of 5×10^{-9} mbar in the analyzer chamber. The detection process included a survey scan to identify the chemical components present and high–resolution scans to detect the levels of certain elements. The spectra are processed though the Multi-Pak Spectrum (Version 9.0) to obtain surface atomic concentrations and all spectra are calibrated using the C 1s spectral peak at 284.8 eV.

3. Results and discussion

3.1. Flotation results

3.1.1. Effect of NH_4Cl on the floatation behavior of pyrite

The effect of pH on the floatability of pyrite is studied and the results are presented in Fig. 3a. As shown in Fig. 3a, in the pH range of 7 to 10, the recovery of pyrite under activation of CAS is apparently lower than that under activation of copper sulfate. This suggests that CAS has a weaker activation effect on pyrite flotation under weakly alkaline conditions. To further explore the effect of NH_4Cl on the flotation of copper-activated pyrite under weakly alkaline conditions, flotation tests of pyrite under activation of CAS (5×10^{-5} mol/L $CuSO_4$ + NH_4Cl) with different NH_4Cl addition are conducted at pH = 9 and the results are shown in Fig. 3b. As seen from Fig.3b, the recovery obviously decreases with the increase of NH_4Cl addition, which further prove that NH_4Cl can reduce the floatability of copper-activated pyrite under weakly alkaline conditions.

3.1.2. Mixed flotation of pyrite and marmatite

The mixed flotation tests of marmatite and pyrite under different activation conditions are conducted (Fig. 4). As shown in Fig. 4, under highly alkaline condition (pH = 12), pyrite is well depressed, but

marmatite is also depressed to some extent. When the pH changed from 12 to 9, the recovery of marmatite increased significantly, but at the same time, the depression of pyrite is deteriorating. After the addition of NH_4Cl, flotation of marmatite is optimized, and the pyrite recovery decreases with the increase of NH_4Cl addition. The mixed flotation test further demonstrates the effectiveness of adding NH_4Cl to improve the separation effect of pyrite and marmatite under weakly alkaline conditions.

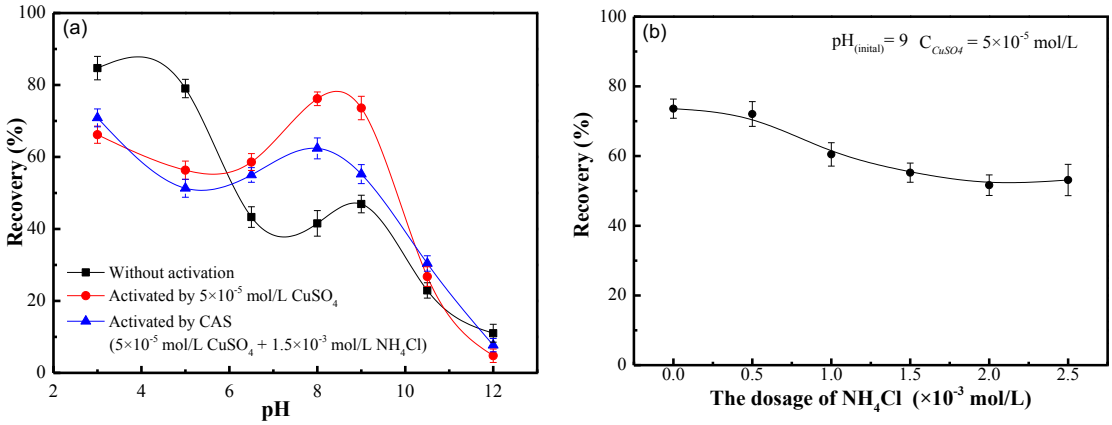

Fig. 3. Effect of (a) pH and (b) NH_4Cl dosage on the floatation behaviour of pyrite ($C_{(KBX)}$ = 10 mg/L)

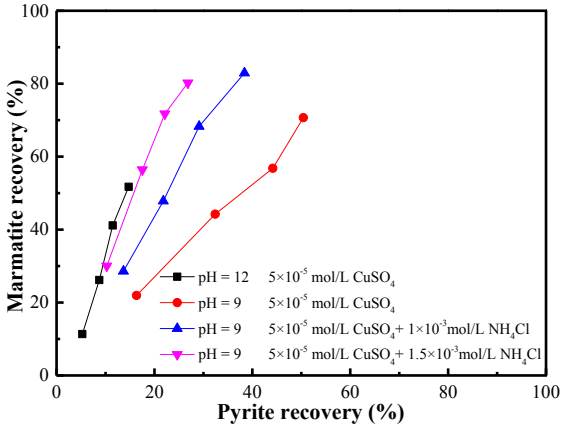

Fig. 4. Effect of pH and NH_4Cl dosage on the separation effect of marmatite and pyrite ($C_{(KBX)}$ = 10 mg/L; the four points on each curve in the graph correspond to the cumulative recovery of marmatite and pyrite in the floated product at 2/4/6/8 min respectively under each flotation condition)

3.2. Adsorption tests

3.2.1. The adsorption of KBX

The adsorption of collector can directly reflect the activation effect of the mineral (Gao et al., 2015). Therefore, the adsorption of KBX on pyrite under different activation conditions are measured to evaluate the effect of NH_4Cl on the copper activation of pyrite (Fig. 5). As seen from Fig. 5, the adsorption amount of KBX basically unchanged in NH_4Cl solution but clearly decreased with increase of NH_4Cl addition. It can be concluded that NH_4Cl itself does not has obvious effect on the flotation of pyrite. But under activation of copper sulfate, NH_4Cl has a significant inhibitory effect on the copper activation process of pyrite.

3.2.2. The adsorption of copper and iron species

Many previous studies (Valdivieso et al., 2004; Boulton et al., 2003) have identified that copper activation products on pyrite surface under alkaline environment are copper sulfides and copper hydroxide. According to the research of Rumball et al. (1996) and He et al. (2005), disodium EDTA can

be used to selectively leach metal oxides, hydroxides, carbonates, and sulfates from sulfide minerals. Therefore, the selective leaching using disodium EDTA is adopted here to separately determine the amounts of adsorbed copper sulfides and copper/iron hydroxides. In the process of leaching, unextracted copper corresponds to copper sulfides and the extracted copper/iron correspond to copper/iron hydroxides.

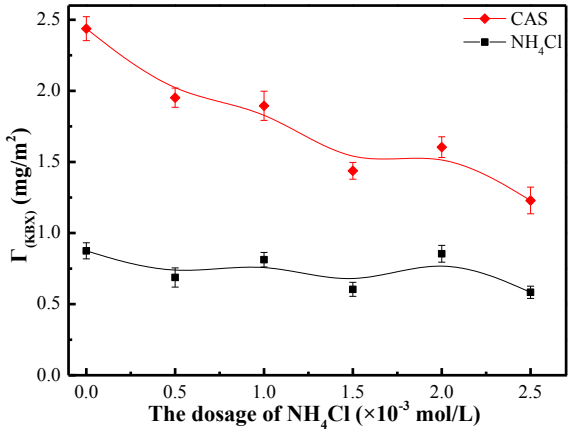

Fig. 5. Effect of NH_4Cl on the adsorption amount of KBX (pH $_{(inital)}$ = 9, C $_{(KBX)}$ = 10 mg/L, CAS = 5×10^{-5} mol/L $CuSO_4$ + NH_4Cl)

3.2.2.1. Effect of NH_4Cl on the adsorption behavior of copper and iron

At pH = 9 (non-buffering system), the amounts of copper adsorbed on pyrite conditioned in copper sulfate and CAS with different NH_4Cl addition are measured, the results are shown in Fig. 6. As seen from Fig. 6, after adding NH_4Cl, the adsorbed amount of the extractable species of copper and iron both increase firstly and then keep steady with the increase of added amounts of NH_4Cl. Conversely, the adsorbed amount of the unextracted species (copper sulfides) decrease with the increase of NH_4Cl addition.

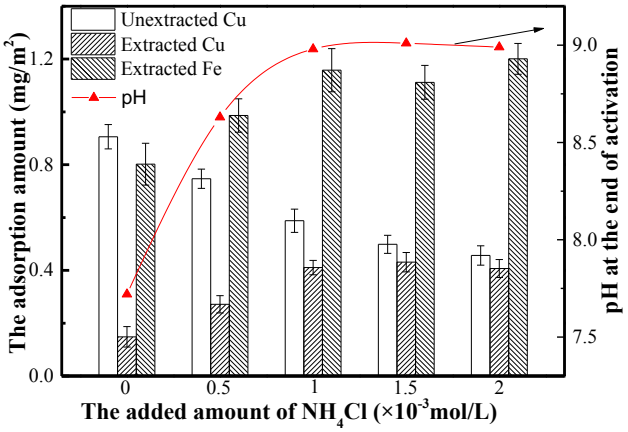

Fig. 6. Effect of NH_4Cl on the adsorption of copper and iron species on the pyrite surface and pH at the end of activation (pH $_{(inital)}$ = 9, C $_{(CuSO4)}$ = 5×10^{-5} mol/L)

The pulp pH decreased from 9 to 7.72 after 5 min of activation by $CuSO_4$. According to the results of previous research (Evangelou and Zhang, 1995), this may be due to the oxidation process of pyrite and the hydrolysis of ferric (Fe^{3+}) or ferrous (Fe^{2+}) ions (as shown in reactions (4-6)). In this test, there is no adjustment of the pH during the stirring process. Therefore, the H^+ released during the oxidation and hydrolysis is sufficient to cause a significant drop in the pH under weakly alkaline conditions.

$$FeS_2 + 7/2\ O_2 + H_2O \rightarrow Fe^{2+} + 2\ SO_4^{2-} + 2\ H^+ \quad (4)$$

$$Fe^{2+} + 1/4\ O_2 + H^+ \rightarrow Fe^{3+} + 1/2\ H_2O \quad (5)$$

$$Fe^{3+} + n\ H_2O \rightarrow Fe(OH)_n(s) + n\ H^+ \ (n = 2 \text{ or } 3) \quad (6)$$

The change in pH is gradually reduced with the increase of the added amount of NH_4Cl. When the added amount is greater than 1×10^{-3} mol/L, the pulp pH after activation basically stabilizes at 9. The above trends in pH after the addition of NH_4Cl may be attributed to the pH buffering property of the conjugated acid-base pair NH_4^+-NH_3. The addition of NH_4Cl leads to the appearance of NH_4^+ and NH_3, and the subsequent pH buffering property maintains a higher solution pH (Stumpp et al., 2012). The change in pH will result in a consequent change in the solution composition, which will further affect the composition of the product formed on the mineral surface. To confirm this from a quantitative perspective, the concentration of Cu^{2+} and the precipitation ratio of copper hydroxide in copper sulfate and CAS are calculated by Visual MINTEQ (Version 3.1), a chemical equilibrium model frequently used in related fields to calculate metal speciation, solubility equilibria, adsorption, etc. in aqueous solution (Sierra et al., 2017; Zuo et al., 2015). The results are shown in Table 2.

Table 2. The comparison of solution compositions of copper sulfate solution and CAS

Solution	pH	Log activity (Cu^{2+})	($M(Cu(OH)_2)/M(Total(Cu))$)%
5×10^{-5} mol/L $CuSO_4$	7.72	-6.15	95.66
5×10^{-5} mol/L $CuSO_4$ +1.5×10^{-3} mol/L NH_4Cl	9.00	-8.71	99.56

As seen from Table 2, although the pH of the system is not much different before and after the addition of NH_4Cl, the activity of Cu^{2+} in the two systems differs by more than 100-fold, and the content of copper hydroxide also has a significant difference. Through the above results of experiment and calculation, it can be concluded that the pH buffering property caused by the addition of NH_4Cl has two significant effects on the copper activation process: on the one hand, the higher pH will cause the result that more hydroxide appears and absorbs on pyrite surface, which can block the adsorption of copper; on the other hand, under higher pH, the lower concentration of Cu^{2+} is not conducive to the activation process.

Further comparison found that when the NH_4Cl addition is more than 1×10^{-3} mol/L (the pH is basically stable at 9), the content of copper hydroxide remains basically unchanged, but the adsorption amount of copper sulfides still shows a clear downward trend. That is, the adsorption amount of copper sulfides is not completely controlled by pH. Therefore, the adsorption behavior of copper under the buffered condition (pH = 9) is studied in Section 3.2.2.2.

3.2.2.2. Effect of NH_4Cl on the adsorption behavior in pH-buffer system

To obtain a stable pH of 9, 5 mL of 0.1 mol/L $Na_2B_4O_7$ is added to the system. The pH after stirring is measured, and the result showed that the pH is still stable at 9. The adsorption amount of copper and iron on mineral surface under the buffered condition of pH = 9 is shown in Fig. 7.

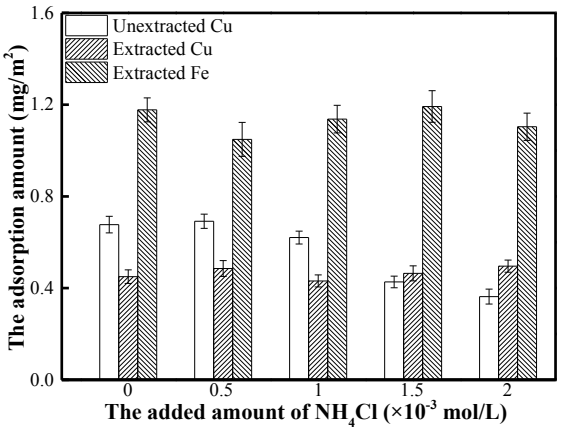

Fig. 7. Effect of NH_4Cl on the adsorption of copper and iron at pH = 9 (buffered system) ($C_{(CuSO4)}$ = 5×10^{-5} mol/L)

As seen from Fig. 7, in the pH buffer system, the amount of the extracted iron and copper do not change significantly, but the adsorption amount of copper sulfides still decreases with increase of NH_4Cl addition. This result again verifies the change trend of the adsorbed amount of copper sulfides in Section 3.2.2.1.

To explore the mechanism behind the above phenomenon from the perspective of solution chemistry, the solution composition of CAS at pH 9 is calculated by Visual MINTEQ, the results are listed in Table 3.

Table 3. The solution composition of CAS (5×10^{-5} mol/L $CuSO_4$ + 1.5×10^{-3} mol/L NH_4Cl) at pH = 9

Components	Concentration (mol/L)	Components	Concentration (mol/L)	Components	Concentration (mol/L)
Cu^{2+}	2.30×10^{-9}	$Cu(OH)_2(aq)$	1.15×10^{-7}	$CuCl^{+}$	5.84×10^{-12}
$Cu(NH_3)^{2+}$	1.29×10^{-8}	$Cu(OH)^{3-}$	4.65×10^{-9}	$CuCl_2(aq)$	2.22×10^{-15}
$Cu(NH_3)_2^{2+}$	1.62×10^{-8}	$Cu(OH)_4^{2-}$	4.28×10^{-13}	$CuCl^{3-}$	3.11×10^{-20}
$Cu(NH_3)_3^{2+}$	5.46×10^{-9}	$Cu_2(OH)^{3+}$	1.07×10^{-15}	$CuCl_4^{2-}$	2.54×10^{-25}
$Cu(NH_3)_4^{2+}$	3.60×10^{-10}	$Cu_2(OH)_2^{2+}$	1.44×10^{-10}	$Cu(HSO_4)^{+}$	1.87×10^{-20}
$CuOH^{+}$	6.47×10^{-8}	$Cu_3(OH)_4^{2+}$	1.42×10^{-11}	$CuSO_4(aq)$	1.88×10^{-11}

It can be seen from Table 3 that the concentration of $Cu(NH_3)_n^{2+}$ (n = 1/2/3) is large than the concentration of Cu^{2+}, which indicates that the extent of the complex reaction of copper and ammonia is significant. Therefore, the explanation for the decrease in the adsorption amount of copper sulfides is the complex reaction of copper and ammonia. The extent ofcomplex reaction is large (the reaction constants are listed in Table 4) and $NH_3(aq)$ competes with the pyrite surface to consume Cu^{2+}, which cut back the amount of copper sulfides formed on the pyrite surface.

Table 4. The equations and constants of complex reaction of copper and ammonia (from Ref. (IUPAC stability constants database, 2001))

Reaction number	Reaction equation	Log K
1	$Cu^{2+} + NH_3 \rightarrow Cu(NH_3)^{2+}$	4.31
2	$Cu^{2+} + 2\,NH_3 \rightarrow Cu(NH_3)_2^{2+}$	7.98
3	$Cu^{2+} + 3\,NH_3 \rightarrow Cu(NH_3)_3^{2+}$	11.02
4	$Cu^{2+} + 4\,NH_3 \rightarrow Cu(NH_3)_4^{2+}$	13.32

Table 5. The treatment conditions of pyrite samples for XPS analyses (pH = 9 (non-buffering system)) and the XPS survey scan results of it

Sample Code	Treatment condition	Content of the surface elements (%)			
		Fe 2p	S 2p	O 1s	Cu 2p
a	deionized water, stirred for 5 min	35.27	56.96	7.77	0.00
b	5×10^{-5} mol/L $CuSO_4$, stirred for 5 min	32.79	51.46	10.05	5.70
c	CAS (5×10^{-5} mol/L $CuSO_4$ + 0.5×10^{-3} mol/L NH_4Cl), stirred for 5 min	29.32	47.37	16.98	6.33
d	CAS (5×10^{-5} mol/L $CuSO_4$ + 1×10^{-3} mol/L NH_4Cl), stirred for 5 min	27.75	42.71	24.29	5.25
e	CAS (5×10^{-5} mol/L $CuSO_4$ + 1.5×10^{-3} mol/L NH_4Cl), stirred for 5 min	28.85	43.59	23.07	4.49

3.3. XPS studies

To verify the reliability of the results of adsorption tests through a more accurate surface inspection method, the XPS analyses are adopted. The XPS spectra and surface atomic ratios of pyrite samples are calculated based on the Multi-Pak Spectrum software (Version 9.0). The conditions of sample processing and the XPS survey scan results are listed in Table 5. It can be seen from the table that the content of O 1s shows a significant upward trend after the addition of NH_4Cl. This implies that more hydroxide is adsorbed on the pyrite surface.

3.3.1. Surface copper analyses

According to the Cu $2p_{3/2}$ binding energies of copper specieson the pyrite surface conditioned under similar conditions given in the literature (Deng et al., 2013), the following two copper species can be identified on surface of these samples: Cu_2S (932.50 eV) and CuO (934.50 eV). CuO may be formed through the dehydration of adsorbed copper hydroxide during the vacuum-drying process (Ghotbi and Rahmati, 2015) and Cu_2S is generated via the reduction of Cu(II) (Ejtemaei and Nguyen, 2017). The peak fitting results for the Cu $2p_{3/2}$ XPS data are shown in Fig. 8, and the corresponding copper content are listed in Table 6. Comparing the composition of copper species on surface of these samples, it can be seen that the relative amount of CuO decreases and the relative amount of Cu_2S increases as the NH_4Cl addition increases.

Table 6. Binding energies and relative contents of different copper species occurring on the surface of pyrite samples conditioned in different solutions

Sample Code	Cu_2S (%)	CuO (%)
	932.50 eV	934.50 eV
b	84.95	15.05
c	77.28	22.72
d	62.23	37.77
e	56.78	43.22

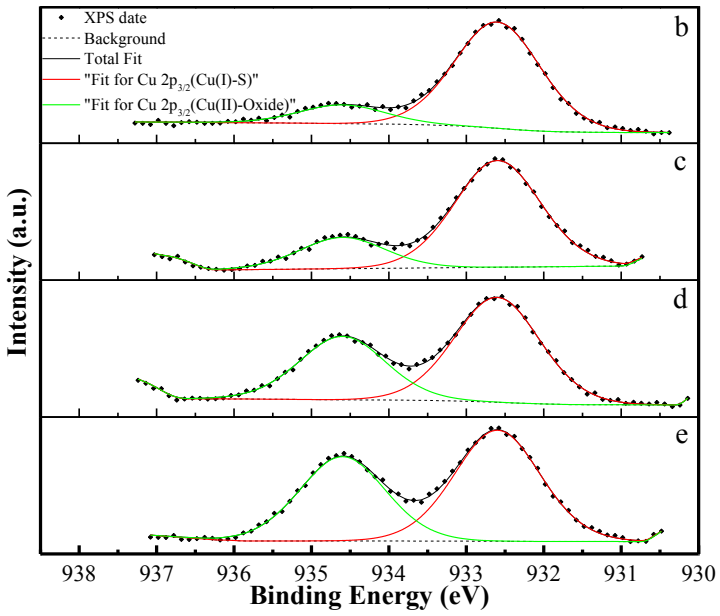

Fig. 8. Cu $2p_{3/2}$ XPS spectra of pyrite conditioned in different solutions: b,c,d and e

3.3.2. Surface sulfur analyses

According to the S 2p binding energies of sulfur specieson the pyrite surface (Ejtemaei and Nguyen, 2017), there are three sulfur species on the unactivated pyrite surface are found: S^{2-} (161.2 eV/162.4 eV),

S^- (bulk) (162.7 eV/163.9 eV) and S_n^{2-} (165.0 eV/166.2 eV). After activation, a new doublet formation at 161.9 eV and 163.1 eV is found, and which corresponds to S^{2-} in the activation product Cu_2S. The peak-fitting results for the S 2p XPS data are shown in Fig. 9, and the corresponding sulfur content is listed in Table 7.

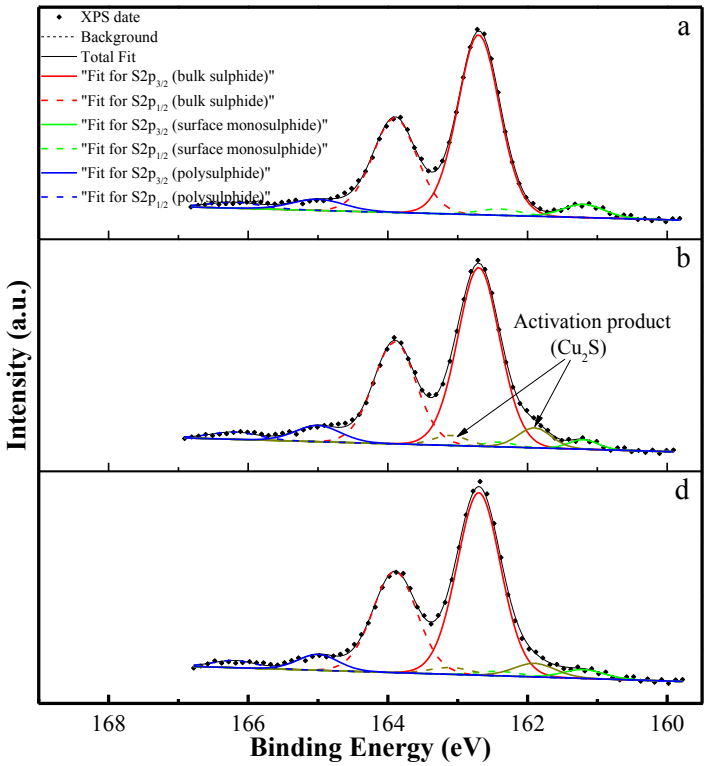

Fig. 9. S 2p XPS spectra of pyrite conditioned in different solutions: a,b and d

Table 7. Binding energies and relative contents of the different sulfur species occurring on the surface of pyrite samples conditioned in different solutions

Sample Code	S^{2-} (%)	Cu_2S (%)	S^- (bulk) (%)	S_n^{2-} (%)
	161.2 eV	161.9 eV	162.7 eV	165.0 eV
a	11.32	0.00	82.33	6.35
b	5.26	12.74	75.20	6.80
c	6.72	10.46	76.94	5.88
d	7.75	8.83	76.50	6.92
e	7.80	8.21	78.13	5.86

The main doublet peaks at 162.7 eV and 163.9 eV are attributed to S^- in the bulk of FeS_2. The polysulphide species (S_n^{2-}) is the polymer formed through the redox of surface sulfur, which frequently appears on the surface of sulfide minerals (He et al., 2005; Ejtemaei and Nguyen, 2017). Pyrite contains both Fe^{2+}-S_2^{2-} bonds and S-S bonds, therefore, the fracture mode of the bond has an important influence on the composition of S species on the pyrite surface. According to the research of Mc Cleverty (1985), the energy required to rupture the S-S bond (< 245 ± 20 kJ/mol) is less than the energy needed to rupture the Fe^{2+}-S_2^{2-} bond (> 300 kJ/mol). Therefore, the weaker S-S bond should be ruptured during the fracture of pyrite and this could produce surface with sulfur monomer (S^-) (Ejtemaei and Nguyen, 2017). However, the S^- is thermodynamically unstable and will further capture electrons from iron to produce monosulphide (S^{2-}) (as shown in reaction (7)), which corresponds to the doublet peaks at 161.2 eV and 162.4 eV (Ejtemaei and Nguyen, 2017).

$$Fe^{2+}{}_{surface} + S^-{}_{surface} \rightarrow Fe^{3+}{}_{surface} + S^{2-}{}_{surface} \quad (7)$$

It can be seen from Table 7 that the content of Cu_2S on the surface is reduced with the increase of NH_4Cl addition. The result of the sulfur analyses is in good agreement with the information obtained from the XPS analyses. This further illustrates the reliability of the results of XPS analyses and the adsorption tests.

4. Conclusions

In this paper, the weakening effect of NH_4Cl on the copper activation of pyrite has been studied and the main conclusions are summarized as follows:

(1) Under weakly alkaline conditions, NH_4Cl has a weakening effect on the activation of pyrite by copper. The addition of NH_4Cl can significantly reduce the floatability of pyrite both in single mineral system, and the mixed mineral system of pyrite and marmatite.

(2) The mechanism of the weakening effect of NH_4Cl on the copper activation of pyrite can be attributed to two aspects: The addition of NH_4Cl leads to the appearance of the conjugated acid-base pair (NH_4^+ and NH_3) and its pH buffering property can impede the decrease in the concentration of OH^-, which results in more hydroxide appearing on pyrite surface; NH_3(aq) can easily react with Cu^{2+} to generate $Cu(NH_3)_n^{2+}$, and it will compete with the pyrite surface to consume Cu^{2+}, which causes a reduction in the amount of copper sulfides formed on the pyrite surface. The increase in the amount of hydrophilic hydroxide and the reduction in the amount of hydrophobic copper sulfides on the surface eventually lead to a weakening in the activation effect of copper on pyrite.

Acknowledgements

The authors would like to acknowledge the financial support provided by the National Natural Science Foundation of China (No. 51764024 & 51764025), Yunnan Applied Basic Research Project (No. 2018FB086)

References

AHMADI, A., RANJBAR, M., SCHAFFIE, M., 2012. *Catalytic effect of pyrite on the leaching of chalcopyrite concentrates in chemical, biological and electrobiochemical systems*. Minerals Engineering, 34.7, 11-18.

BOULTON, ADRIAN, DANIEL FORNASIERO, AND J. RALSTON., 2005. *Effect of iron content in sphalerite on flotation*. Minerals engineering, 18(11), 1120-1122.

BUCKLEY, A. N., HOPE, G. A., LEE, K. C., PETROVIC, E. A., WOODS, R., 2014. *Adsorption of o-isopropyl-n-ethyl thionocarbamate on cu sulfide ore minerals*. Minerals Engineering, 69, 120-132.

BULUT, G., CEYLAN, A., SOYLU, B., GOKTEPE, F., 2012. *Role of starch and metabisuphite on pure pyrite and pyritic copper ore flotation*. Physicochemical Problems of Mineral Processing, 48(1), 261902-92104.

BOULTON, A., FORNASIERO, D., & RALSTON, J., 2001. *Depression of iron sulphide flotation in zinc roughers*. Minerals Engineering, 14(9), 1067-1079.

BICAK, O., EKMEKCI, Z., BRADSHAW, D. J., HARRIS, P. J., 2007. *Adsorption of guar gum and CMC on pyrite*. Minerals Engineering, 20(10), 996-1002.

BIDARI, E., & AGHAZADEH, V., 2015. *Investigation of copper ammonia leaching from smelter slags: characterization, leaching and kinetics*. Metallurgical & Materials Transactions B, 46(5), 1-10.

BOULTON, A., FORNASIERO, D., RALSTON, J., 2003. *Characterisation of sphalerite and pyrite flotation samples by XPS and TOF-SIMS*. International Journal of Mineral Processing, 70(1), 205-219.

DENG, M., KARPUZOV, D., LIU, Q., XU, Z., 2013. *Cryo-xps study of xanthate adsorption on pyrite*. Surface and Interface Analysis, 45(4), 805-810.

DÁVILA-PULIDO, G. I., URIBE-SALAS, A., ESPINOSA-GÓMEZ, R., 2011. *Comparison of the depressant action of sulfite and metabisulfite for cu-activated sphalerite*. International Journal of Mineral Processing, 101(1), 71-74.

EJTEMAEI, M., & NGUYEN, A. V., 2017. *Characterisation of sphalerite and pyrite surfaces activated by copper sulphate*. Minerals Engineering, 100, 223-232.

EVANGELOU, V. P., ZHANG, Y. L., 1995. *A review: pyrite oxidation mechanisms and acid mine drainage prevention*. CRC Critical Reviews in Environmental Control, 25(2), 141-199.

GUO, B., PENG, Y., ESPINOSA-GOMEZ, R., 2015. *Effects of free cyanide and cuprous cyanide on the flotation of gold and silver bearing pyrite*. Minerals Engineering, 71, 194-204.

GAO, Z., SUN, W., HU, Y., 2015. *New insights into the dodecylamine adsorption on scheelite and calcite: an adsorption model*. Minerals Engineering, 79, 54-61.

GHOTBI, M. Y., RAHMATI, Z., 2015. *Nanostructured copper and copper oxide thin films fabricated by hydrothermal treatment of copper hydroxide nitrate*. Materials & Design, 85, 719-723.

HE, S., FORNASIERO, D., SKINNER, W.,2005. *Correlation between copper-activated pyrite flotation and surface species: effect of pulp oxidation potential*. Minerals Engineering, 18(12), 1208-1213.

IUPAC stability constants database, 2001. *Sc–database and mini–scdatabase*, Timble, UK: Academic Software.

JIANG, C. L., WANG, X. H., PAREKH, B. K., LEONARD, J. W., 1998. *The surface and solution chemistry of pyrite flotation with xanthate in the presence of iron ions*. Colloids and surfaces a physicochemical and engineering aspects.

LEPPINEN, J. O., 1990. *FTIR and flotation investigation of the adsorption of ethyl xanthate on activated and non-activated sulfide minerals*. International Journal of Mineral Processing, 30(3), 245-263.

MEHRABANI, J. V., MOUSAVI, S. M., NOAPARAST, M., 2011. *Evaluation of the replacement of nacn with acidithiobacillus ferrooxidans in the flotation of high-pyrite, low-grade lead–zinc ore*. Separation & Purification Technology, 80(2), 202-208.

MCCLEVERTY, J., 1985. *Inorganic-Chemistry - Principles of Structure and Reactivity, 3rd Edition – Huheey, Je*. Nature, 314, 30–30.

PENG, Y., WANG, B., GERSON, A., 2012. *The effect of electrochemical potential on the activation of pyrite by copper and lead ions during grinding*. International Journal of Mineral Processing, 102(s 102–103), 141-149.

QIN, W., JIAO, F., SUN, W., HE, M., HUANG, H., 2012. *Selective flotation of chalcopyrite and marmatite by mbt and electrochemical analysis*. Industrial & Engineering Chemistry Research, 51(35), 11538-11546.

RUMBALL, J. A., & RICHMOND, G. D., 1996. *Measurement of oxidation in a base metal flotation circuit by selective leaching with EDTA*. International Journal of Mineral Processing, 48(1), 1-20.

SHEN, W. Z., FORNASIERO, D., RALSTON, J., 2001. *Flotation of sphalerite and pyrite in the presence of sodium sulfite*. International Journal of Mineral Processing, 63(1), 17-28.

SHEN, W. Z., FORNASIERO, D., RALSTON, J., 1998. *Effect of collectors, conditioning pH and gases in the separation of sphalerite from pyrite*. Minerals Engineering, 11(2), 145-158.

STUMPP, M., HU, M. Y., MELZNER, F., GUTOWSKA, M. A., DOREY, N., & HIMMERKUS, N., et al, 2012. *Acidified seawater impacts sea urchin larvae pH regulatory systems relevant for calcification*. Proceedings of the National Academy of Sciences,109(44), 18192-18197.

SIERRA, J., ROIG, N., GIMÉNEZ, P. G., PÉREZ-GALLEGO, E., SCHUHMACHER, M., 2017. *Prediction of the bioavailability of potentially toxic elements in freshwaters. comparison between speciation models and passive samplers*. Science of the Total Environment, 605-606, 211.

VALDIVIESO, A. L., CERVANTES, T. C., SONG, S., CABRERA, A. R., LASKOWSKI, J. S., 2004. *Dextrin as a non-toxic depressant for pyrite in flotation with xanthates as collector*. Minerals Engineering, 17(9), 1001-1006.

XIAOJUN, X., & Ş. KELEBEK, 2000. *Activation of xanthate flotation of pyrite by ammonium salts following it's depression by lime*. Developments in Mineral Processing, 13, C8b-43–C8b-50.

ZUO, M., RENMAN, G., GUSTAFSSON, J. P., RENMAN, A., 2015. *Phosphorus removal performance and speciation in virgin and modified argon oxygen decarburisation slag designed for wastewater treatment*. Water Research, 87, 271-281.